

# **Analysis of hydraulic resistance of soil surface seals in relation to sediment particle size**

## **ABSTRACT**

Surface sealing, and their role in runoff and erosion, especially, in agricultural fields have been recognized as major set-backs to irrigation operations. Though the process is restricted to only the topmost soil layer of some few millimetres in depth, surface sealing can substantially impede the infiltration of water into the soil. However, information on this process is much less documented. The aim of this study was to investigate the possible relationships between seal type and hydraulic resistance. The paper presents a simple theoretical approach which allows the estimation of changes in hydraulic resistance at the soil surface as a function of time following the formation of surface seals formed from different sediment particles at different concentrations in suspension. A laboratory column studies was designed to investigate the effects of water quality on infiltration rate. Clear water, and muddy water comprising sand, silt and clay at different concentrations of 10, 20, 30 and 40 g in 400 cm<sup>3</sup> of water were used as the test fluids.

*Keywords: Slaking, Surface seal, Hydraulic conductivity, Hydraulic resistance, Infiltration*

## **1. INTRODUCTION**

Slaking of soil aggregates with resultant surface sealing are common characteristics of many cultivated soils, especially, in arid and semi-arid areas [1]. These processes of soil slaking and sealing are the result of the kinetic impact of raindrops on the soil surface and the translocation of soil particles by flowing water. Accordingly, Zejun et al. [2] reported that rainfall causes a series of interactions between water and soils: compaction, disintegration, detachment, entrainment and deposition. These actions result in the formation of seal, and subsequently the crust of soils. The formation of seal depends on many factors, including the texture and stability of the soil, intensity and energy of rainfall, gradients and length of slope, and electrolyte concentration of the soil solution and rainwater [3]. The extent of surface sealing has been reported to be highly dependent on soil texture, with the silt content being a good indicator of the soil's susceptibility [1, 4]. Upon deposition, the translocated particles could clog soil pores and form superficial layers characterised by higher bulk density and lower saturated hydraulic conductivity than the soil beneath [1, 5]. In this regard, surface seal formation can be viewed to result from three [6 – 8]:

- 1) Physical disintegration of soil aggregates and their compaction, caused by the impact of raindrops.
- 2) Chemical dispersion of the clay particles. The low electrical conductivity of the rainwater as well as the organo-chemical bonds between the primary particles of the surface aggregates, dictate the rate and degree of dispersion.
- 3) An interface suction force which arranges suspended clay particles into a continuous dense layer. Such almost impermeable layers form right on the surface of the soil or in the immediate subsurface washed-in layer, as discussed by McIntyre [9].

Soil seals can significantly reduce infiltration rate and subsequently lower the utilization of water resources, and increase runoff, which result in soil erosion. This is so because the saturated hydraulic conductivity of the sealed surface is always lower than that of the subsurface [8]. Due to the loss of soil water storage and infiltration capacities, soil erosion and flooding are significantly increased [1]. The reduction in infiltration rate under sealed conditions is controlled by the surface seal rather than the water content of the soil profile [10]. The objectives of this study were to measure the effect of surface seal formation from different sediment particles on infiltration under field conditions, and to develop a technique to quantify the hydraulic resistance of the developing seal. The technique would be useful for the management of irrigation practices in Ghana.

### **1.1 Theory**

According to Segeren and Trout [10], the most direct method to simulate the process of soil surface sealing is to model a two-layer soil profile in which the seal is the top layer. In this case, the hydraulic

conductivity of the seal  $K_x(d)$  is measured as a function of time. From Darcy's law, the conductivity of the seal, which is a function of the particle diameter of the sediment [1] can be calculated as [10]:

$$K_x(d) = -q \left( \frac{Z_x}{\Delta m + \Delta g} \right) \quad (1)$$

During transient state flow under unsaturated conditions, we assume that the matric potential gradient across the seal is larger than the gravitational gradient, hence, the gravitational component can be neglected and equation (1) reduces to:

$$K_x(d) = -q \left( \frac{\Delta m}{\Delta g} \right) \quad (2)$$

However, during steady state flow under saturated conditions, we assume a unit hydraulic gradient. Therefore, equation (1) could be expressed as:

$$K_x(d) = q \quad (3)$$

where,

$Z_x$  = Seal thickness [L]

$q$  = Flux through the soil [L/T]

$\Delta g$  = Change in gravitational potential across the seal [L]

$\Delta m$  = Change in matric potential across the seal [L]

$d$  = Soil particle diameter

$K_x(d)$  = Hydraulic conductivity of the surface seal [L/T] given as [1]:

$$K_x(d) = \left( \frac{K_s}{c} \right) d_* \quad (4)$$

$K_s$  = Hydraulic conductivity of the initial soil surface [L/T]

$c$  = Concentration of soil sediment in suspension [M/L<sup>3</sup>]

$d_*$  = Dimensionless particle diameter of sediment defined as [1, 11]:

$$d_* = d \left[ \sqrt[3]{\left( \frac{\rho_f g \rho_\gamma}{\omega^2} \right)} \right] \quad (5)$$

where,

$\rho_\gamma$  = Submerged particle density [ML<sup>-3</sup>], expressed as:  $\rho_s - \rho$

$\rho_f$  = Fluid density [ML<sup>-3</sup>]

$g$  = Acceleration due to gravity [LT<sup>-2</sup>]

$\omega$  = Dynamic viscosity [ML<sup>-1</sup>T<sup>-1</sup>]

Since seal thickness is highly variable with time and is difficult to measure directly, the most convenient method to measure this parameter is given by modification of the relation by Tuffour et al. [1]:

$$Z_x = cK_x(d)t + cV_s t \quad (6)$$

$V_s$  = Settling velocity of sediment [L/T], defined as the downward velocity in a low dense fluid at equilibrium in which the sum of the gravity force, buoyancy force and fluid drag force are equal to zero [12, 13]. According to Stokes' law, the fall velocity of spherical particles with Reynolds number (Re) less than 1, can be calculated from [8, 14]:

$$V_s = \frac{1}{18} \frac{g(s-1)D^2}{\mu} \quad (7)$$

where,

$g$  = Acceleration due to gravity [L/T<sup>2</sup>]

$s$  = Relative density ( $\rho_s/\rho$ )  
 $\mu$  = Kinematic viscosity [ $L^2/T$ ]  
 $t$  = Time [T]

Swartzendruber [15] defined the hydraulic resistance  $R_h$ [T] of the seal to describe the resistance of the seal to flow regardless of thickness as:

$$R_h = \frac{Z_x}{K_x(d)} = \frac{ct(K_s + V_s)}{\left(\frac{K_s}{c}\right) d_*} \quad (7)$$

The assumptions proposed for this study require that all soil properties with influence on infiltration remain constant for the sub seal layer [10]. In addition to the assumptions proposed by Tuffour and Bonsu [16], the following assumptions were also proposed for the method employed in the study [1, 11, 17]:

1. The seal does not form instantly, but upon formation, it is saturated from the start.
2. The hydraulic resistance  $R_h$  is the only soil hydraulic property that changes after the start of infiltration.
3. Flux through the soil is uniform.

## 2. MATERIALS AND METHODS

### 2.1 Collection and description of soil samples

Soil samples described by FAO-UNESCO (1988) [18] as Gleyic Arenosol were collected from an arable field in the Department of Horticulture, Kwame Nkrumah University of Science and Technology, Kumasi, Ghana. The soils have high proportion of large pores owing to their coarse texture, which accounts for high aeration, rapid drainage slow runoff and low moisture holding capacity [19]. Twenty five (25) core samples were randomly collected samples from 0-20 cm soil depth were collected from 25 different spots [8]. Undisturbed soil cores were collected from the field site using a 10 cm diameter PVC sewer pipe cut to a length of 30 cm and bevelled at the outer part of the lower end to provide a cutting edge to facilitate the insertion of the core. Field cores were collected by first digging a circular trench around an intact "pillar" of undisturbed soil which was taller and had a slightly larger diameter than the core sampler. The core sampler was then inserted directly into the pillar of soil by striking a wooden plank positioned across the top of the ring, with a mallet. By this, the edges of the pillar were allowed to fall away from the core as it was inserted. Following complete insertion the core was excavated by hand. When taking the soil core the inner ring created an air filled annulus, hence a sealant was used to ensure good contact between the soil and core and thereby minimised any edge flow down the core. Therefore, the air gaps between the soil and inner surface of the core were filled with melted petroleum jelly (Vaseline was used in this case).

### 2.2 Laboratory analyses of soil samples

The hydrometer method [20] was used in the determination of the particle size distribution. Soil water content was determined on volume basis before and after the laboratory infiltration tests. Moist soil samples were collected from the field two days after a heavy rainfall when the soil was assumed to be at or near field capacity, [8, 21]. The saturated hydraulic conductivity ( $K_s$ ) measurements were made on the cores in the laboratory using the modified falling head permeameter method similar to that described by Bonsu and Laryea [8, 22].

### 2.3 Separating soil particles

The different soil particles were obtained by dry sieving through a series of graduated sieves with different mesh sizes as described by Tuffour [8], and Tuffour and Abubakari [23]. The soil samples were shaken over nested sieves (in a decreasing order from top to bottom) (Figure 1), which were selected to furnish the information required by specification. During sieving, the sample was subjected to a tap mechanism (i.e., both vertical movement or vibratory sieving and horizontal motion or horizontal sieving) for approximately 120 minutes to provide complete separation of the fine (i.e. dispersible) soil

particles of the order 0.05 mm for fine sand, 0.02 mm for silt and < 0.002 mm (assumed herein as 0.001 mm) for clay, according to FAO classification.



**Figure 1: Sieves arranged in a stack with the mesh size increasing from bottom to top on mechanical shaker**Source: Tuffour [8]

### 2.3 Experimental verification of the model

The performance of the proposed model was verified with a series of ponded infiltration tests with clear and muddy water as described in Tuffour and Bonsu [16], and Tuffour et al. [1]. Laboratory infiltration studies were conducted with a series of ponded infiltration tests for 60 minutes with clear water, and muddy water made of suspensions of different soil particle diameters, viz., fine-sand, clay and silt obtained from the soil separation process, at different concentrations. The different concentrations were made by adding clean (distilled) water to, 10 (T1), 20 (T2), 30 (T3) and 40 g (T4) of soil to make a total of 400 cm<sup>3</sup> and dispersed in a mechanical shaker for 60 minutes. Additionally, an infiltration test was conducted with distilled water (T5), which served as a reference for the study. The ponded infiltration experiments were conducted with a surface ponded thickness of 5 cm. A plastic sheet was used to cover the surface of the soil as the suspension was being added, in order to prevent disturbance of the surface. The plastic sheet was removed and a flexible tubing, which had already been filled with water, was used to connect the surface of the suspension to a constant head device. A piezometer in the form of a flexible tubing was connected to a manometer and allowed measurement of the cumulative volume of infiltration. The vertical infiltration was measured in the soil column for 60 minutes. The initial infiltration was measured at 30 seconds interval for the first five minutes after which the interval was increased to 60, 180 and 300 seconds, respectively, as the process slowed down towards the steady state. To compute the cumulative infiltration amount (*I*) from the experiment, the volume of water was converted to depth from the relation:

$$I = \frac{Q}{A}$$

where,

*Q* = Cumulative volume of water (ml); 1 ml = 1 cm<sup>3</sup>

*A* = Surface area of the ring, given by:

$$A = \pi r^2$$

$$r = \frac{1}{2} \text{ Ring diameter}$$

The cumulative infiltration amounts (*I*) were plotted as a function of time for each run on a linear scale with GraphPad Prism 6.0. The slopes of the cumulative infiltration amounts taken at different time scales represented the infiltration rates (*i*), which were plotted against time and the steady state

infiltrability ( $K_o$ ) was obtained at the point where the infiltration rate curve became almost parallel to the time axis [24, 25].

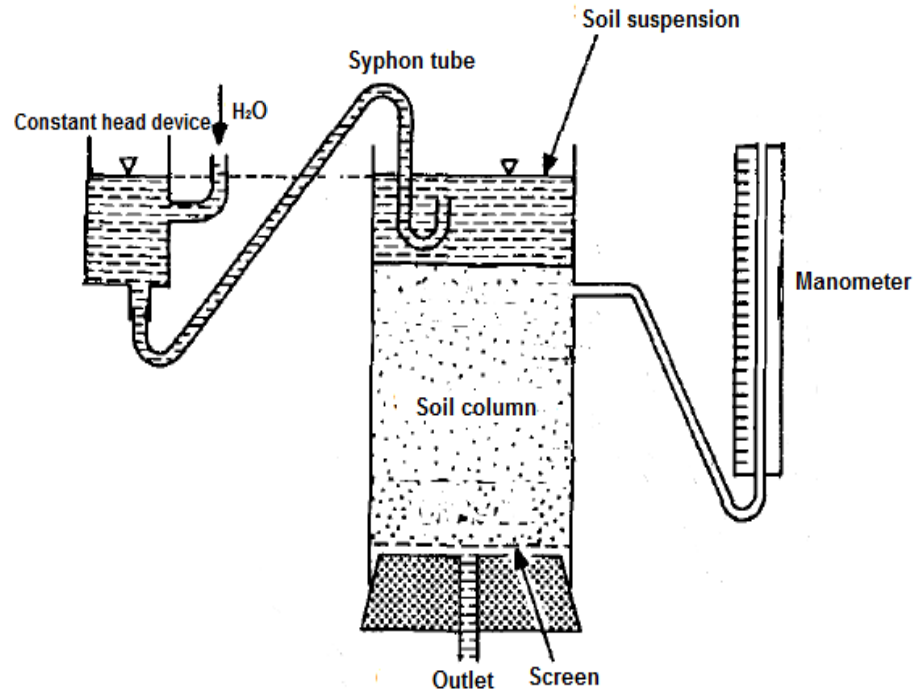


**Figure 2:** A schematic diagram of the apparatus used to test the theory Source: Tuffour [8]

### 3. RESULTS AND DISCUSSIONS

The results of initial analysis of soil physical and hydraulic properties of the study area are presented in Table 1. The results showed that the texture of the field surface (0 - 20 cm) was loamy sand, with sand, silt and clay fractions of 84%, 4.30% and 11.70%, respectively. The average bulk density was 1.34 g/cm<sup>3</sup> with total porosity of 49.43%. The average antecedent and saturated moisture contents were 23.58% and 47.70%, respectively. The average saturated hydraulic conductivity was  $2.5 \times 10^{-3}$  mm/s. Table 2 presents the summary of the results of the measured physical and hydraulic properties after the infiltration experiment. Detailed discussions on the comparison between Tables 1 and 2 are reported in Tuffour and Abubakari [23]. In this study, changes in soil physical properties that affected infiltration were assumed to occur at the soil surface in the form of a thin surface seal. For the no-seal columns, (i.e., columns run by clear water), cumulative infiltration was successfully predicted from the initial saturated-hydraulic-conductivity of the soil [16]. Thus, structural changes of the soil columns as they wetted under sediment-movement conditions, including aggregate sloughing and soil consolidation [10, 16], actually affected infiltration as evidenced by the differences in parameter values in Tables 1 and 2. The study also emphasizes the possibility that, with sediment movement and surface seal formation, physical changes may occur below the seal layer.

With consideration of the mass balances of sediment particles, the flux of suspension through the soil column was captured through infiltration measurements and thickness of a surface seal. Seal thickness from the different sediment particles as estimated from equation (6) as presented in Table 1 varied widely between sand and the finer sediments (clay and silt). However, no clear differences were observed between those of clay and silt. In addition, Figures 3 – 5 show that hydraulic resistance has a linear relationship with seal thickness, in that, an increase in seal thickness results in an increase in hydraulic resistance of the seal. Thus, increases in sediment concentration which eventually results in high seal thickness would be expected to result in seal hydraulic resistance by cursory analysis. However, a close observation of the results clearly showed that clay seals which produced lowest seal thickness had the greatest hydraulic resistance than sandy textured seals, which had the highest seal thickness as presented in Table 3. In addition to these discrepancies, silt

seals, which had similar thickness as clay seals had the lowest hydraulic resistance. Thus, hydraulic resistance and infiltration rates followed the same pattern as total infiltration rates, that is, higher as crust development increased, except for the lichen crust on fine-textured soils, which generated steady state infiltration rates similar to the PSC.

**Table 1: Summary of initial soil physical and hydraulic properties**

| Soil property   | Number of samples | Mean value |
|---|-------------------|------------|
| Saturated hydraulic conductivity ( $\text{mm s}^{-1}$ ) | 5                 | 2.50E-03   |
| Bulk density ( $\text{g cm}^{-3}$ )                     | 5                 | 1.34       |
| Total porosity (%)                                      | 5                 | 49.43      |
| Volumetric moisture content (%)                         | 5                 | 23.58      |
| Saturated moisture content (%)                          | 5                 | 47.70      |
| Moisture deficit (%)                                    | 5                 | 24.12      |
| Sand (%)  | 5                 | 84.00      |
| Silt (%)  | 5                 | 4.30       |
| Clay (%)  | 5                 | 11.70      |
| Texture   | 5                 | Loamy sand |

227 **Table 2: Summary of soil physical and hydraulic properties after infiltration**

| Soil property                  | Fluid       |                              |        |        |        |                              |        |        |        |                                   |        |        |        |
|--------------------------------|-------------|------------------------------|--------|--------|--------|------------------------------|--------|--------|--------|-----------------------------------|--------|--------|--------|
|                                | Clear water | Clay suspension <sup>s</sup> |        |        |        | Silt suspension <sup>s</sup> |        |        |        | Fine sand suspension <sup>s</sup> |        |        |        |
|                                |             | 10                           | 20     | 30     | 40     | 10                           | 20     | 30     | 40     | 10                                | 20     | 30     | 40     |
| $K_s$ (mm s <sup>-1</sup> )    | 2.5E-3      | 1.0E-4                       | 5.0E-5 | 3.3E-5 | 2.5E-5 | 2.0E-3                       | 1.0E-3 | 6.7E-4 | 5.0E-4 | 5.0E-3                            | 2.5E-3 | 1.7E-3 | 1.3E-3 |
| $\rho_b$ (g cm <sup>-3</sup> ) | 1.34        | 1.37                         | 1.45   | 1.53   | 1.55   | 1.37                         | 1.43   | 1.48   | 1.52   | 1.36                              | 1.41   | 1.45   | 1.47   |
| $f$ (%)                        | 49.43       | 48.30                        | 45.28  | 42.26  | 41.51  | 48.30                        | 46.04  | 44.15  | 42.64  | 48.67                             | 46.79  | 45.28  | 44.53  |
| $\theta_v$ (%)                 | 23.58       | 21.01                        | 19.28  | 17.28  | 16.65  | 21.74                        | 20.44  | 19.21  | 18.04  | 22.53                             | 21.38  | 19.61  | 18.97  |
| $\theta_s$ (%)                 | 47.70       | 43.50                        | 42.60  | 40.90  | 40.10  | 45.00                        | 44.40  | 43.50  | 42.30  | 46.30                             | 45.70  | 43.30  | 42.60  |

228 <sup>s</sup>Mass of sediment particles in suspension (g);  $\theta_v$  (%) = Volumetric water content at field capacity;  $\rho_b$  (g cm<sup>-3</sup>) = Bulk density;  $f$  (%) = Total  
 229 porosity;  $\theta_s$  (%) = Saturated water content;  $K_s$  (mm s<sup>-1</sup>) = Saturated

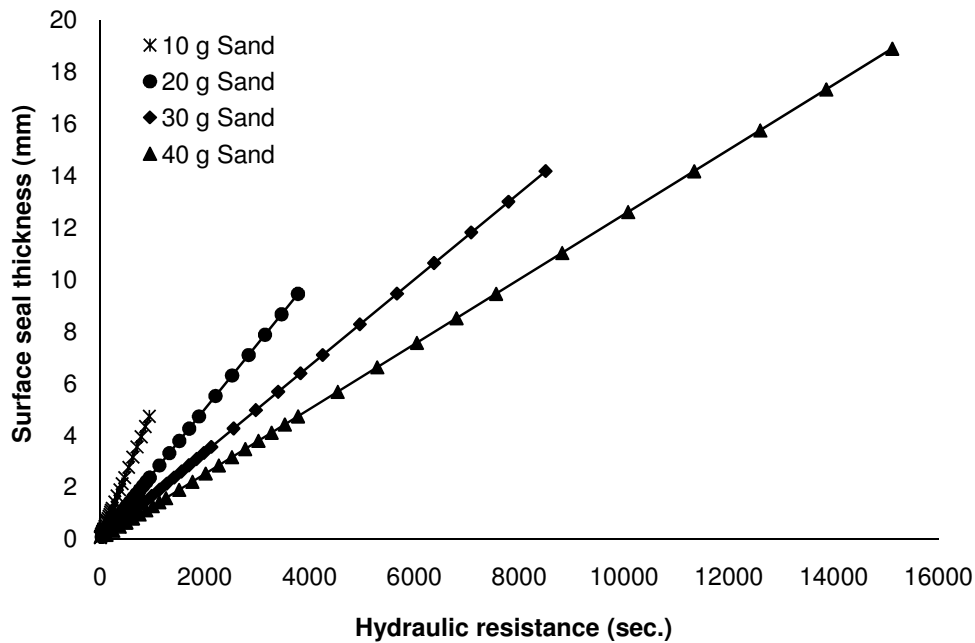
230 **Table 3: Estimated seal thickness for the different sediment particles at various concentrations in suspension**

| Time (S) | Seal thickness (mm)          |          |          |          |                              |          |          |          |                              |          |          |          |
|----------|------------------------------|----------|----------|----------|------------------------------|----------|----------|----------|------------------------------|----------|----------|----------|
|          | Clay suspension <sup>s</sup> |          |          |          | Silt suspension <sup>s</sup> |          |          |          | Sand suspension <sup>s</sup> |          |          |          |
|          | 10                           | 20       | 30       | 40       | 10                           | 20       | 30       | 40       | 10                           | 20       | 30       | 40       |
| 30       | 1.875E-3                     | 3.750E-3 | 5.625E-3 | 7.500E-3 | 1.875E-3                     | 3.751E-3 | 5.626E-3 | 7.502E-3 | 3.750E-3                     | 7.500E-3 | 1.125E-2 | 1.500E-2 |
| 300      | 1.875E-2                     | 3.750E-2 | 5.625E-2 | 7.500E-2 | 1.876E-2                     | 3.751E-2 | 5.626E-2 | 7.502E-2 | 3.750E-2                     | 7.500E-2 | 1.125E-1 | 1.500E-1 |
| 600      | 3.750E-2                     | 7.500E-2 | 1.125E-1 | 1.500E-1 | 3.751E-2                     | 7.502E-2 | 1.125E-1 | 1.500E-1 | 7.500E-2                     | 1.500E-1 | 2.250E-1 | 3.000E-1 |
| 900      | 5.625E-2                     | 1.125E-1 | 1.688E-1 | 2.250E-1 | 5.626E-2                     | 1.125E-1 | 1.688E-1 | 2.251E-1 | 1.125E-1                     | 2.250E-1 | 3.375E-1 | 4.500E-1 |
| 1800     | 1.125E-1                     | 2.250E-1 | 3.375E-1 | 4.500E-1 | 1.125E-1                     | 2.251E-1 | 3.376E-1 | 4.501E-1 | 2.250E-1                     | 4.500E-1 | 6.750E-1 | 9.000E-1 |
| 2100     | 1.313E-1                     | 2.625E-1 | 3.938E-1 | 5.250E-1 | 1.313E-1                     | 2.626E-1 | 3.939E-1 | 5.251E-1 | 2.625E-1                     | 5.250E-1 | 7.875E-1 | 1.0500   |
| 2700     | 1.688E-1                     | 3.375E-1 | 5.063E-1 | 6.750E-1 | 1.688E-1                     | 3.376E-1 | 5.064E-1 | 6.752E-1 | 3.375E-1                     | 6.750E-1 | 1.0125   | 1.350    |
| 3000     | 1.875E-1                     | 3.750E-1 | 5.625E-1 | 7.500E-1 | 1.876E-1                     | 3.751E-1 | 5.626E-1 | 7.502E-1 | 3.750E-1                     | 7.500E-1 | 1.125    | 1.500    |
| 3600     | 2.250E-1                     | 4.500E-1 | 6.750E-1 | 9.000E-1 | 2.251E-1                     | 4.501E-1 | 6.752E-1 | 9.002E-1 | 4.500E-1                     | 9.000E-1 | 1.350    | 1.800    |

231 <sup>s</sup>Mass of sediments in suspension (g)



232 The surface sealing process could be viewed to have resulted from a filtration process,  
 233 wherein, there was a phase transition of the sediments from the flowing fluid phase into a  
 234 solid phase upon settling on the soil surface or in the pore spaces [26, 27]. Two main  
 235 mechanisms could explain this filtration process – Transport of fluidized sediments with  
 236 characteristic size larger than the size of the pore constrictions of the pore network was  
 237 not possible. This implies that the sediment material was blocked and settled only at the  
 238 soil surface (i.e., the occurrence of pore clogging was restricted only at the surface), as  
 239 could be depicted for the coarse fragments. On the other hand, in the case of the smaller  
 240 fluidized sediments relative to the pore constrictions, transport depended solely on the  
 241 hydraulic conditions (i.e., hydraulic gradient) of the soil column[27]. Of these, high  
 242 concentrations of suspended sediment, irrespective of its characteristic diameter  
 243 appeared to promote sealing capacity, with increasing seal thickness and hydraulic  
 244 resistance. Herein, the sealing capacity was observed to be high for sediments with  
 245 smaller diameter. This is a clear indication that thesealing process is related to the  
 246 geometrical properties of the porous medium and of the sediments [26, 27].  
 247



248  
 249 **Figure 3: Relationship between surface seal thickness and hydraulic resistance of**  
 250 **sand particles**

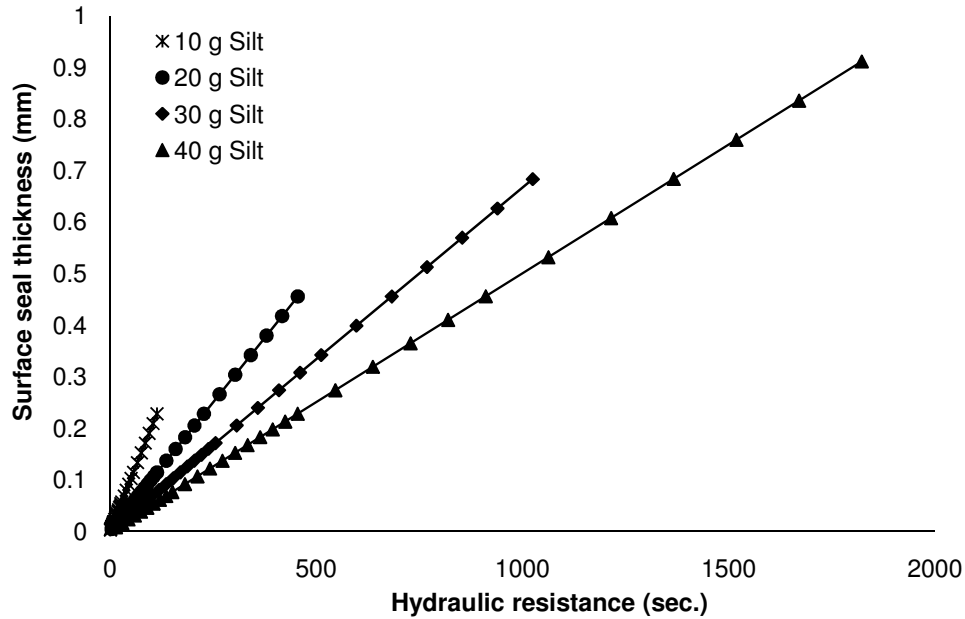


Figure 4: Relationship between surface seal thickness and hydraulic resistance of silt particles

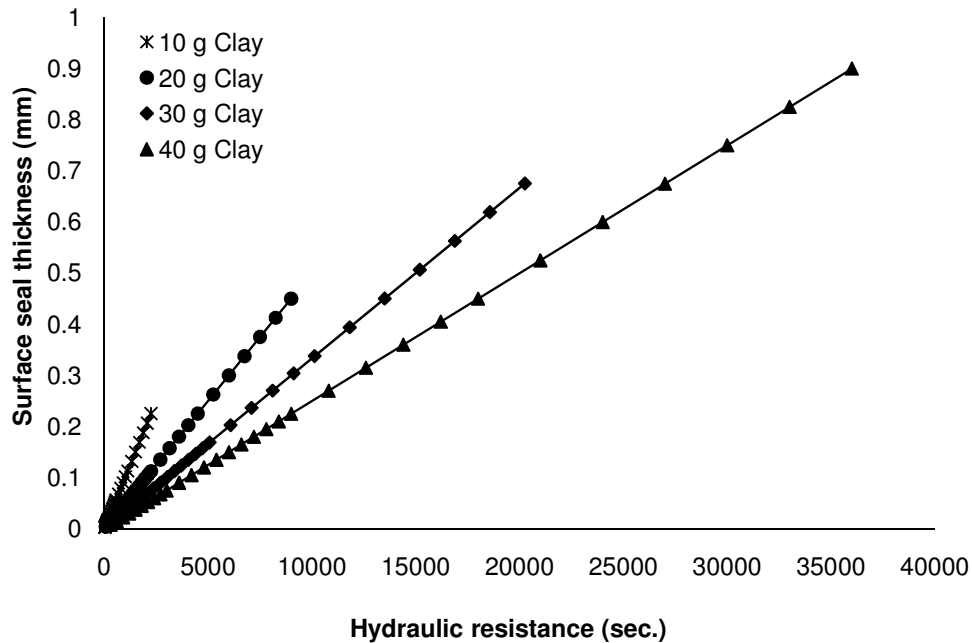


Figure 5: Relationship between surface seal thickness and hydraulic resistance of clay particles

It is clear from Figures 3 – 5 that increasing seal thickness results in increasing hydraulic resistance for the different seal types. At lower sediment concentrations, seal thicknesses were low with corresponding low hydraulic resistance. Thus, hydraulic resistance increased with increasing surface seal development. The type (i.e. texture) of

seal significantly influenced hydraulic resistance which consequently affected infiltration parameter values [16]. As can be seen in Figures 3 – 5, the clay seal showed the highest seal hydraulic resistance, which eventually produced lower infiltration parameters as reported by [16]. Thus, the seals from coarse-textured sediments produced high infiltration parameter values, whereas those from fine-textured soils, produced lower infiltration parameters [16]. A detailed report on the effects of sediment particles in infiltrating water is provided in Tuffour and Bonsu [16], wherein, fine sediments in irrigation water have shown a very high capability of soil surface seal formation with associated significant reduction in infiltration rates. It is interesting to note that the methodology employed herein for the infiltration experiment does not preclude the likelihood that, with sediment movement and surface seal formation, physical changes occur below the thin surface layer. Sealing processes including consolidation and washing-in of sediment particles, which can reduce conductivity below the seal are reflected in the seal hydraulic resistance values estimated in this study [10]. A study by Segeren and Trout [10] on the effects of surface seal resistance on water infiltration revealed that infiltration, relative to infiltration with no seal, versus seal resistance were best fitted by exponential decay functions. In this regard, with seal resistance of zero (no effect of the seal on infiltration), the relative infiltration would be 1.0, and will curve arbitrarily closely to zero as the seal resistance increases. For instance, doubling the resistance from 0.1 to 0.2 resulted in only a 25% decrease in the infiltration rate, due to the increase in potential gradient across the seal as the resistance increased.

The depositional layer densities and saturated hydraulic conductivities for the various sediments were assumed constant for each concentration. However, the characteristic thickness for the different sediment concentrations varied with time. The continuing gradual increase in hydraulic resistance during the infiltration process as observed in Figures 3 – 5 was as a result of the seal formation. This implies that the seal resistance continued to increase throughout the process. From the study, it is evident that although infiltration is directly related to the conductivity of the seal, the relationship is not proportional, as might be assumed from a cursory analysis [8]. Thus, a relative decrease in infiltration requires a larger relative increase in the seal hydraulic resistance [10]. Accordingly, Glanville and Smith [27] reported that in sealed soils, the surface seal rather than the water content of the soil profile determines the reduction in the infiltration rate. This report also clearly highlights the role of seal resistance in water infiltration. From the study, it is evident that seal hydraulic resistance can be estimated fairly well by applying Darcy's law to measured potentials and infiltration rate, which provides a very efficient comparative evaluation of the effect of management practices on surface seal formation [10].

Theoretically, hydraulic conductivity is commonly employed as a very useful parameter than hydraulic resistance in soil hydrology. This is in view of the fact that the surface seal thickness, which difficult to determine experimentally is expected to increase with time during the infiltration process. This makes the computation of hydrological processes difficult when seal hydraulic resistance is employed in numerical studies. Under real field conditions, the infiltrating water is a fluid comprising a mixture of soil sediment particles and undispersed aggregates, and irrigation and/or rainfall water [28]. These soil materials of varying sizes, masses, settling velocities and concentrations undergo differential settling, which results in a surface seal composed of different layers; Each layer assumes a characteristic hydraulic conductivity [28], which is a function of the particle size of the seal forming sediment [1, 8, 16]. Thus, the effective seal could be composed of several layers with varying conductivities [10, 28]. Since the net effect of the seal on infiltration is a function of the ratio of the seal conductivity and the seal thickness [10], their variations will be very essential in soil hydrology. Consequently, hydraulic resistance (is a more practical and useful parameter than hydraulic conductivity to characterize the effects of the seal on infiltration [1, 8, 10, 16].

#### 4. CONCLUSIONS

Observations and measurements from the study showed that surface sealing, seal thickness and seal hydraulic resistance were highly dependent on the characteristics of soil sediments and fluid. Thus, the diameter of the sediment in suspension strongly affected the development of surface seals. Seal thickness, hitherto, estimated visually with the aid of a microscope on soil cores after infiltration studies was determined by a simple model proposed in an earlier study by author. Additionally, sediment concentration also greatly affected the surface sealing process, as well as seal conductivity, seal thickness and seal resistance. Moreover, the study has revealed that, during the formation of surface seals, the seal thickness increases with time and sediment concentration, irrespective of the sediment diameter, which can have marked influence in reducing infiltration rates. In this regard, surface seal hydraulic resistance can be a very useful parameter to describe the effects of surface seals on infiltration process in soils and the key effect of sealing in increasing surface runoff and the potential for erosion was made obvious from the study results.

#### REFERENCES

- [1] Tuffour HO, Bonsu M, Quansah C & Abubakari A. A physically-based model for estimation of surface seal thickness. *International Journal of Extensive Research*. 2015; 4: 60-64.
- [2] Zejun T, Tingwu L, Qingwen Z & Jun Z. The Sealing Process and Crust Formation at Soil Surface under the Impacts of Raindrops and Polyacrylamide. 12th ISCO Conference. 2002; 456-462.
- [3] Remley PA & Bradford JM. Relationship of soil crust morphology to interrill erosion parameters. *Soil Science Society of America Journal*. 1989; 53: 1215-1221.
- [4] Norton LD. Micromorphological study of surface seals developed under simulated rainfall. *Geoderma*. 1987; 40: 127-140.
- [5] Betzalel I, Morin J, Benyamini Y, Agassi M, Shainberg I. Water drop energy and soil seal properties. *Soil Science*. 1995; 159: S. 13-22.
- [6] Agassi M, Shainberg I & Morin J. Effect of electrolyte concentration and soil sodicity on the infiltration rate and crust formation. *Soil Science Society of America Journal*. 1981; 45: 848-851.
- [7] Morin J, Benyamini Y & Michaeli A. The dynamics of soils crusting by rainfall impact and the water movement in the soil profile. *Journal of Hydrology*. 1981; 52: 321-335.
- [8] Tuffour HO. Physically based modeling of water infiltration with soil particle phase. Ph.D. Thesis, Kwame Nkrumah University of Science and Technology, Kumasi, Ghana. 2015.
- [9] McIntyre DS. Permeability measurements of soil crust formed by raindrop impact. *Soil Science*. 1958; 85: 185-189.
- [10] Segeren AG & Trout TJ. Hydraulic resistance of soil surface seals in irrigated furrows. *Soil Science Society of America Journal*. 1991; 55: 640-646.
- [11] Dietrich WE. Settling velocity of natural particles. *Water Resource Research*. 1982; 18: 1615-1626.
- [12] She K, Trim L & Pope D. Fall velocities of natural sediment particles: a simple mathematical presentation of the fall velocity law. *Journal of Hydraulic Research*. 2005; 43(2): 189-195.
- [13] Wu W & Wang SSY. "Formulas for sediment porosity and settling velocity." *Journal of Hydraulic Engineering*. 2006; 132(8): 858-862.
- [14] Cheng NS. Simplified settling velocity formula for sediment particle. *Journal of Hydraulic Engineering ASCE*. 1997; 123(2): 149-152.
- [15] Swartzendruber D. Water flow through a soil profile as affected by the least permeable layer. *Geophysical Research*. 1960; 65: 4037-4042.
- [16] Tuffour HO & Bonsu M. Application of Green and Ampt Equation to infiltration with soil particle phase. *International Journal of Scientific Research in Agricultural Sciences*. 2015; 2(4): 76-88.

379 [17] Moore ID. Effects of surface sealing on infiltration. Transactions of American Society  
380 of Agricultural Engineers. 1981; 24: 1546-1552.

381 [18] FAO-UNESCO. Soil map of the world, 1:5,000,000. Revised Legend. 4th draft. 1988.

382 [19] Adu SV. Soils of the Kumasi Region, Ashanti Region, Ghana. Soil Research  
383 Institute, CSIR, Ghana. Memoir 8: pp. 81-85. 1992.

384 [20] American Society for Testing Materials (ASTM). Standard test method for particle  
385 size analysis of soils. D422-63(1972). 1985 Annual Book of ASTM Standards.  
386 American Society for Testing and Materials, Philadelphia, 04.08: pp. 117-127. 1985.

387 [21] MotsaraMR & Roy RN. Guide to laboratory establishment for plant nutrient analysis.  
388 FAO Fertilizer and Plant Nutrition Bulletin.2008; 19: 31-33.

389 [22] Bonsu M &Laryea KB. Scaling the saturated hydraulic conductivity of an Alfisol.  
390 Journal of Soil Science. 1989; 40: 731-742.

391 [23] Tuffour HO & Abubakari A. Effects of water quality on infiltration rate and surface  
392 ponding/runoff. Applied Research Journal.2015. 1(3): 108-117.

393 [24] Tuffour HO, Bonsu M &Khalid AA. Assessment of soil degradation due to  
394 compaction resulting from cattle grazing using infiltration parameters. International  
395 Journal of Scientific Research in Environmental Sciences.2014a; 2(4): 139-149.

396 [25] Tuffour HO, Bonsu M, Khalid AA & Adjei-Gyapong T. Scaling approaches to  
397 evaluating spatial variability of saturated hydraulic conductivity and cumulative  
398 infiltration of an Acrisol. International Journal of Scientific Research in  
399 Knowledge.2014b;2(5): 224-232.

400 [26] Schaufler A, Becker C, Steeb H & Scheuermann A. A continuum model for infiltration  
401 problems. ICSE6 Paris - August 27-31, 2012; 663-670.

402 [27] Glanville SF & Smith GB. Aggregate breakdown in clay soils under simulated rain  
403 and effects on infiltration. Australian Journal of Soil Research. 1988; 9: 668-675.

404 [28] Tuffour HO. Analysis of infiltration through a stratified surface seal. Unpublished.